RESEARCH ARTICLE-PETROLEUM ENGINEERING

Performance Improvement of the Surfactant Polymer Flooding Using Bio Synthesized Calcium Carbonate Nanoparticles: An Experimental Approach

Himanshu Kesarwani[1] · Fahad Khan[1] · Apoorv Tandon[1] · Reza Azin[2] · Shahriar Osfouri[3] · Shivanjali Sharma[1]

Abstract

Injection of chemicals in the reservoir in order to displace the remaining oil from the pore spaces is among the most widely accepted techniques. Combination of surfactant and polymer along with nanoparticles (NPs) is gaining the attention of scholars nowadays. Present work focuses on the application of bio-Ca NPs with the surfactant polymer (SP) slug to improve its efficiency. Surface tension, interfacial tension, surfactant adsorption and oil recovery were examined for the evaluation of performance of the NPs-assisted SP injection technique. Addition of 1000 ppm of NPs reduced the CMC of surfactant by 24%. Synergistic effect between bio-Ca NPs and anionic surfactant molecules observed from the experimental results of surface tension and IFT values. The surface tension value of distilled water reduces to 34.5 mN from 72.6 mN/m upon addition of 2500 ppm surfactant. Addition of NPs further reduced the surface tension of the solution by 24%. Introduction of NPs modified the wetting behavior of oil-wet surface to strongly water-wet surface. Furthermore, addition of NPs also improved the viscosity of the SP slug by 41% at 108 s^{-1} shear rate. An increase in cumulative oil recovery from $\sim$69 to $\sim$76% was obtained upon addition of 1000 ppm of bio-Ca NPs in SP slug. Furthermore, 1000 ppm of NPs addition also reduced the surfactant adsorption by 33% for 1000 ppm of surfactant concentration. It can be inferred from the experimental data that the bio-Ca NPs has the potential to improve the performance of the chemical injection technique that can be exploited for additional oil recovery.

Keywords Contact angle · Interfacial tension (IFT) · Surfactant adsorption · Oil recovery

Abbreviations

A	Adsorption of surfactant
S_i	Initial concentration of surfactant
S_f	Final concentration of surfactant
M_s	Mass of solution
M_r	Mass of adsorbent added in surfactant solution

N_{ca}	Capillary number
μ_w	Injection fluid viscosity
v	Injection fluid velocity
σ_{ow}	Interfacial tension between the injection and displaced fluid
Φ	Porosity of the sand column
S_{wi}	Connate water saturation
S_{oi}	Initial oil saturation
S_{or}	Residual oil saturation
Z_{avg}	Average hydrodynamic diameter
R^2	Coefficient of determination
Q_o	Concentration of solid phase in equilibrium
K_{ad}	Langmuir adsorption constant
n	Freundlich adsorption parameter
K_f	Freundlich adsorption constant
B	Temkin adsorption parameter
K_i	Temkin adsorption constant

✉ Shivanjali Sharma
  ssharma@rgipt.ac.in

[1] Department of Petroleum Engineering and Geo Engineering, Rajiv Gandhi Institute of Petroleum Technology, Jais 229304, India

[2] Department of Petroleum Engineering, Faculty of Petroleum, Gas and Petrochemical Engineering, Persian Gulf University, Bushehr, Iran

[3] Department of Chemical Engineering, Faculty of Petroleum, Gas and Petrochemical Engineering, Persian Gulf University, Bushehr, Iran

1 Introduction

Oil and gas industry needs new technologies in order to compete with the rising energy demands. Enhanced oil recovery (EOR) propounds promising answers to the same. EOR processes often include the injection of chemicals which augment the reservoir natural energy for effective oil displacement. These chemicals alter the physiochemical properties of the reservoir and its fluids to create favorable conditions for oil production [1]. With further advancement in EOR processes, more recovery can be achieved. The introduction of nanoparticles (NPs) in EOR process has proved to be a turning point in improving the recovery factor by enhancing its sweep efficiency. The introduction of NPs with surfactant polymer (SP) flooding [2], a subset of chemical enhanced oil recovery (CEOR) is being investigated in present study. Surfactant helps in lowering IFT which leads to increase the capillary number. Also, surfactant addition tends to modify the wetting behavior of the rock whereas polymer addition amplifies injection fluid viscosity, thereby reducing the mobility ratio and providing better sweep efficiency. The combined effect of surfactant and polymer makes it one of the most efficient CEOR [3]. However, SP flooding also have few drawbacks of which loss of surfactants on the rock surface is the major. Because of the adsorption, efficiency of surfactant to balance IFT reduces. Surfactant loss can be reduced by introducing some additives with the surfactant solution such as polymer, alkali or NPs [4].

Introduction of NPs in the petroleum industry for the enhanced recovery factor is not new. NPs have been known to alter the various reservoir and injection fluid properties. NPs can modify the physical properties of reservoir rocks such as wettability alteration [5–7], changes in properties of fluids [8], improvement in trapped oil displacement [9], plugging the pore channels which is caused by the mechanisms of mechanical entrapment and log jamming. As the pore channels, being in micron-scale are much bigger than nanoparticles therefore it can easily enter the pore channel and agglomerate at the entry of the pore throat causing surge in pressure and flow of trapped oil. Apart from this, nanoparticles have resistance to degradation at high temperature and salinity, which makes them a suitable ingredient for addition in surfactant solutions to improve the recovery of oil in harsh reservoir conditions [10].

It has been proved earlier that NPs can enhance the efficacy of the CEOR [11–15]. Although there are a lot of mechanisms which explain the oil mobilization with NPs injection. Adsorption of NPs on the surface to minimize IFT [16], pH alteration [17], disjoining pressure [18] and wettability modification [19] are among the most discussed mechanism that involves the addition of NPs. Various nanofluid has been used to improve the oil displacement from the pore spaces. Giraldo et al, in their research, have used alumina-based nanofluids for sandstone cores and have concluded that nanofluids can alter its wettability. This resulted in improved efficacy of anionic surfactant with low NPs concentration and yielded higher oil recovery [20]. Rezk et al have performed experiments to understand the effect of silica NPs with sodium dodecyl sulfate (SDS) surfactant [21]. They found that SiO_2 NPs altered the wettability of glass surface and improved the sweep efficiency by 13%. Hu et al have examined the effect of rutile TiO_2 NPs on water (brine) flooding and have inferred that low NPs concentrations provide better oil mobilization [22]. Approximately 40% of additional oil recovery was obtained corresponding to only 20 ppm NPs concentration. Ju and Fan have reported that the wettability of sandstone surfaces can be modified from oleophilic to hydrophilic by adsorption of lipophobic and hydrophilic polysilicon NPs [23]. Suleimanov and co-workers have discussed the role of adding NPs with surfactant on the wettability, surface tension and adsorption of the surfactant. A synergistic impact of the NPs with the surfactant on various properties was observed [24]. Bayat et al have used three metal oxide NPs (Al_2O_3, TiO_2 and SiO_2) for improving the oil recovery through a limestone sample and found that the adsorption tendency of the NPs on the limestone surface follows the order $SiO_2 > TiO_2 > Al_2O_3$ [25]. Moghaddam and co-workers experimentally examined the impact of eight NPs on oil recovery and have found an incremental oil recovery of approximately 9% with $CaCO_3$ NPs [26].

It can be inferred from the earlier studies that nanoparticles could improve the production of hydrocarbon, yet the major obstacle of NPs agglomeration remains consistent. Agglomeration of NPs in colloids solution increases the particle size of NPs suspended in the liquid phase and this eventually leads to the settling of NPs. Apart from this, commercial NPs are toxic for plants and environment and are also non-biodegradable. In order to overcome this problem, present work uses bio-Ca NPs which are very easily dispersed in the solution and after ultra-sonication for 10 min forms a stable suspension solution. Moreover, unlike commercial nanoparticles, bio-Ca NPs are biosynthesized, biodegradable and non-toxic to plants and environments. Having such advantages, these nanoparticles have an edge over relatively costly, non-environmentally friendly, toxic and non-biodegradable conventional nanoparticles. The production of NPs from biological resources is now widely implemented [27, 28], as they have shown significant applications in various areas like developing anti-cancer drugs [9], drug delivery systems [29] and formation of scaffolds for bone repair and tissue engineering [30]. The bio-Ca NPs used in present study are synthesized from bone of cuttlefish, found in Persian Gulf of the order *Sepiida* and belong to *Cephalopoda* class. The cuttlebone is majorly composed of Calcium Carbonate and *Chitin*. The performance of these bio-Ca NPs on the wettability alteration of rock surface was examined and it was

observed that they have the potential to change the carbonate rock wettability from being oil-wet to water-wet [31]. Apart from that, these NPs have been reported to be of low cost and environmentally friendly in nature [32]. Because of these specific properties, the authors have identified bio-Ca NPs as a potential additive for the conventional SP flooding to enhance its performance. Furthermore, application of bio nanoparticles in oil and gas industry is not yet investigated deeply. Hence, this study would provide an idea about the performance evaluation of the oil mobilization potential using bio-Ca nanoparticles and various mechanisms involved for the wettability reduction, IFT stabilization and surfactant adsorption reduction.

The present study involves the measurement of the surface tension of various concentrations of the NPs solutions. The synergistic effect of the anionic surfactant and the NPs on the IFT, surface tension and wettability modification ability was explored. Further, the efficiency of NPs in decreasing the amount of surfactant loss at the solid sand crystals was studied. Finally, the oil displacement efficiency of the NPs -ssisted SP flooding was examined by carrying out the sand pack flooding.

2 Experimental Section

2.1 Materials

Sodium dodecyl sulfate (SDS) having purity > 99% and molecular weight of 288.38 g/mol was taken from Molychem Pvt. Ltd, India. Polyacrylamide (PAM) used for flooding operation was obtained from SNF Floerger a chemical industry company based in France. The crude oil from Oil and Natural Gas Corporation (ONGC), Ankaleshwar field, India was used in flooding operation has a viscosity of 5.5 cP at temperature of 333 K and acid number of 1.25 mg KOH/g. The physical property of the crude oil used in the experiment is given in Table 1. Toluene used in flooding operation has purity > 99% was obtained from Rankem Chemicals. Sodium chloride with molecular formula NaCl and having purity > 99% was taken from Merck chemicals. The sand pack and sand powder pellet were prepared using normal beach sand after washing and drying in a hot air oven at 383.15 K in order to remove the moisture. Deionized water used in the experiment was collected from Elga lab water purifier had a resistivity of 18.1 MΩ.cm. The Cuttlebone, *Sepia Pharaonis*, used for bio-Ca NPs, was collected along the northern bank of the Persian Gulf in Bushehr coastal area.

2.2 Synthesis of Bio-Ca NPs

The bio-Ca NPs were produced after several steps [31]. At the first step, the cuttlebones collected from Persian Gulf

Table 1 The physical properties of crude oil

S. No	Property	Value
1	Pour Point (°C)	22
2	Flash Point (°C)	117
3	Wax Content (%)	20
4	Asphaltene (%)	6.6
5	Acid content (mg/KOH)	1.25
6	Viscosity at 333 K (cp)	5.5

northern coastal zone were washed to remove sand and clay using deionized water and dried in an oven (Memmert, Germany) overnight at 105 °C. After that, the cuttlebones were crushed in a ceramic mortar and sieved through a 25 mesh to get the residue. In the third step, the initial bio-Ca powder was placed in a high-energy planetary ball mill (NARYA-MPM-2*200H, Iran) under the argon atmosphere to avoid degradations of the particles. The ball-powder mass ratio was set as 10 and the rotational speed at 340 rpm. In order to avoid the rise in temperature during milling process, the machine was stopped for 15 min after each 30 min run. This milling process was repeated 8 times for producing bio-Ca NPs, and a brief summary of the whole process was illustrated in Fig. 1. The physical properties of the bio-Ca NPs were presented in Table 2 [32]. The synthesized bio-Ca nanoparticles were characterized by FESEM technique using JEOL JSM 7900F (Fig. S1). The elemental analysis of the same using EDX technique is given in Table S1. Thermal stability of the nanoparticles was examined by performing the TGA experiments (Fig. S2).

2.3 Surface Tension Measurement

Surface tension of a fluid may be defined as the characteristic of liquid surface to resist external forces. The surface tension values of various concentrations of test samples (0–8000 ppm of surfactant) were measured using surface tensiometer (KYOWA DY-500) with the help Du-Nouy ring method. The equipment has an accuracy of 0.02 mN/m. The ring used was having diameter of 14.5 mm and thickness of 0.4 mm and was properly cleaned before testing and three readings were taken to check the repeatability. Interfacial tension (IFT) between the crude oil and different test samples was also measured using the same method. 50 ml of test sample was taken in a beaker and 20 ml of crude oil was carefully poured above the sample surface carefully to make the interface between the immiscible fluids. The CMC value was obtained by measuring surface tension of varying concentration of surfactant solution. The concentration corresponding to minimum surface tension value gives the CMC of surfactant.
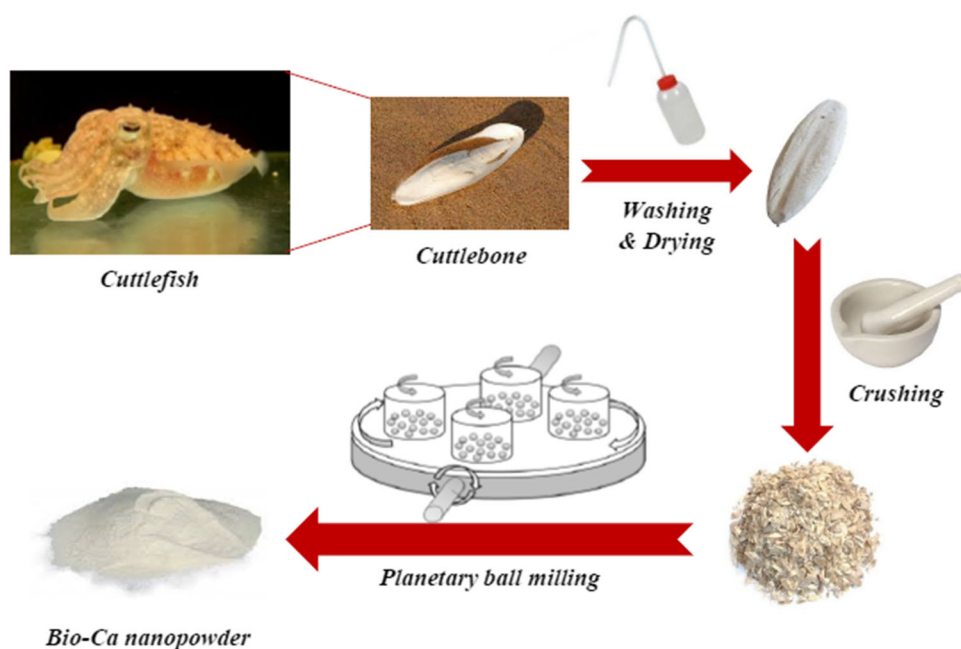
Fig. 1 Bio-Ca nanopowder
production process

Table 2 The physical properties
of bio-Ca NPs [32]

Purity (%)	Mean particle diameter (nm)	Specific surface area (m²/g)	Status	Color	True density (g/cm³)
>98	40–50	13.7	Solid	White to yellow	3.1

2.4 Contact Angle Measurement

The impact of the bio-Ca NPs on the wetting properties of the rock surface was examined by measuring the contact angle value with the help of sessile drop method. The assembly consists of a D-CAM Engineering syringe pump, an evacuated chamber and a camera. Similar methodology has been used in our previous studies [15, 33]. A sand pellet using the clean powdered sand particles was prepared using the hydraulic press load of 25 tons for 10 s. A layer of crude oil was applied on the pellet and left for 2 days to ensure its oil wetting nature. The solution sample was dropped on sand pellet surface with the help of the syringe pump at a flow rate of 0.06 mL/hr. The pellet was kept in the evacuated chamber. The fluid coming from the needle forms a sessile drop as it reaches to the surface and an image is captured using the camera. The captured picture was examined using software ImageJ to get the contact angle [34]. The experiments were conducted at room temperature and pressure conditions. All the flow lines were properly cleaned with deionized (DI) water and a picture of DI water was analyzed after every measurement to ensure no impurity in the system. Each experiment was repeated thrice to check the repeatability of the results. The equipment has an accuracy of 1 degree.

2.5 Dynamic Light Scattering (DLS)

DLS provides size distribution profile of diminutive particles suspended in a fluid. As the size of NPs is very critical in the formulation of the chemical slug to be used for oil recovery process. Hence, DLS studies for bio-Ca NPs suspended in distilled water were performed using Malvern Zetasizer Nano-ZS instrument. The average hydrodynamic diameter and zeta potential of these bio-NPs were measured. The instrument uses a cuvette in which the sample was taken (~ 1.4 mL). A coherent and monochromatic light source (laser beam of 633 nm wavelength) is passed through the transparent cuvette hitting the small particles. The scattering intensity of these particles fluctuates over time which undergoes through Brownian motion and with the help of Stokes–Einstein equation the size of particle is calculated. The cuvette was thoroughly cleaned using methanol and dried after each measurement and sample was prepared with caution to prevent dust and a syringe filter (0.2 μm) was applied to remove larger impurities. The temperature was maintained at 30 °C and the equilibrium time of 120 s was provided to establish an equilibrium temperature throughout.

2.6 Viscosity Measurement

Viscosity is an important rheological property, which is measured to understand the characteristics and deforma-

tion of a sample with respect to shear rate and temperature. The sample viscosities were studied using modular compact rheometer of Anton Paar (MCR-52). It has a double gap pressure cell geometry with 32.000 mm of cup outer diameter and 60.000 mm of bob length. The inner diameter of bob was 32.800 mm and outer diameter was 35.120 mm. The test was conducted at three temperatures (30, 60 and 90 °C) and the shear rate was varied from 4.24 to 4240 s^{-1} in order to understand the viscosity at various shear rates. The test was conducted without pressurizing the system. All the parts of the assembly of the rheometer (cup and bob) were properly cleaned and dried each time with the help of deionized water both at beginning and end of measurement.

2.7 Flooding Experiments

Impact of bio-Ca NPs on the oil mobilization was studied by conducting forced imbibition experiments on a sand pack. The sand pack used for the experiment has a radius of 1.27 cm, while the length of sand pack was 30 cm. The schematic diagram of the setup can be seen in Fig. 2. The setup comprises of an injection syringe pump capable of delivering 10,000 psi, procured from D-CAM Engineering, Ahmedabad, four accumulators (500 mL) each containing crude oil, water, toluene and chemical slugs. The temperature of the setup was set at a constant value of 60 °C to imitate the reservoir conditions. Injection of fluid was done at a constant rate (60 mL/hr) during the whole flooding process with the help of a syringe pump. Normal beach sand particles of 40–60 US mesh (250–400 microns) were used for the experiment. Sand pack preparation was done by ramming down sand particles inside the sand pack holder along with the gradual addition of known amount of 1 wt% NaCl solution. At the start of the experiment, water was injected in the sand pack and the absolute permeability and porosity were determined using Darcy's law when the steady-state flow was achieved. After that, crude oil was pushed in the sand pack, which displaced some water out of the sand column. By measuring the amount of water displaced from the sand pack and volume of water used while ramming the sand particles for sand column preparation, connate water, and initial oil saturation were determined. The flow lines were properly rinsed by running toluene through them, then sand pack was left for 6 days to convert the wetting behavior of sand particles towards oil-wet [35]. Further, water injection process was performed to imitate water flooding and obtain secondary oil recovery. All displacements were conducted horizontally to minimize the impact of gravity forces. The pressure drop between the ends of sand column and produced volumes of oil and water were recorded with respect to displacing fluid volume. After secondary recovery, 50% pore volume (PV) of chemical slug was pumped inside the sand column in order to displace the left oil. Further, chase water

was injected through the sand column till no oil drop could be produced from the sand column. The chemical slug comprised of a mixture of 2500 ppm of surfactant and 1000 ppm of polymer in which NPs concentration was varied from 0 to 1000 ppm.

2.8 Surfactant Adsorption

Adsorption of the surfactant molecules at the rock surface was evaluated in a similar way as done by previous researchers [36, 37]. 20 mL of surfactant solutions with varying concentrations of bio-Ca NPs from 100 to 1000 ppm were prepared. The samples were tested for the conductivity using a conductivity meter (Labman Scientific Instruments Multiparameter LMMP-30). 2 g of sand particles of 250 μm size were mixed in the surfactant solution and left undisturbed for about 24 h. A characteristic curve for each concentration of bio-Ca NPs mixed with different concentrations of the surfactant solution was made. After that, the solution was kept in a centrifuge (Medifuge, ThermoFisher) at 4500 rpm for 15 min in order to separate the sand from surfactant solution. Then the conductivity of the samples was checked again. The corresponding characteristic curve was used in measurement of the volume of surfactant adsorb on sand surface after the separation. The concentration of the surfactant before and after the separation of the sand particles was noted and their difference was calculated. The reduction in the surfactant concentration gave an estimate of the surfactant loss due to its adsorption on sand particles. The mass of sand mixed in the surfactant solution per unit volume of solution was kept constant. All measurements were carried out at 30 °C and 14.7 psi. The adsorption of surfactant molecule was determined by Eq. 1:

$$A = \frac{\left\{ \left(S_i - S_f \right) \times \frac{M_s}{M_r} \right\}}{1000} \qquad (1)$$

where,

A is loss of surfactant in mg/g.

S_i is initial concentrations of surfactant in ppm.

S_f is final concentrations of surfactant in ppm.
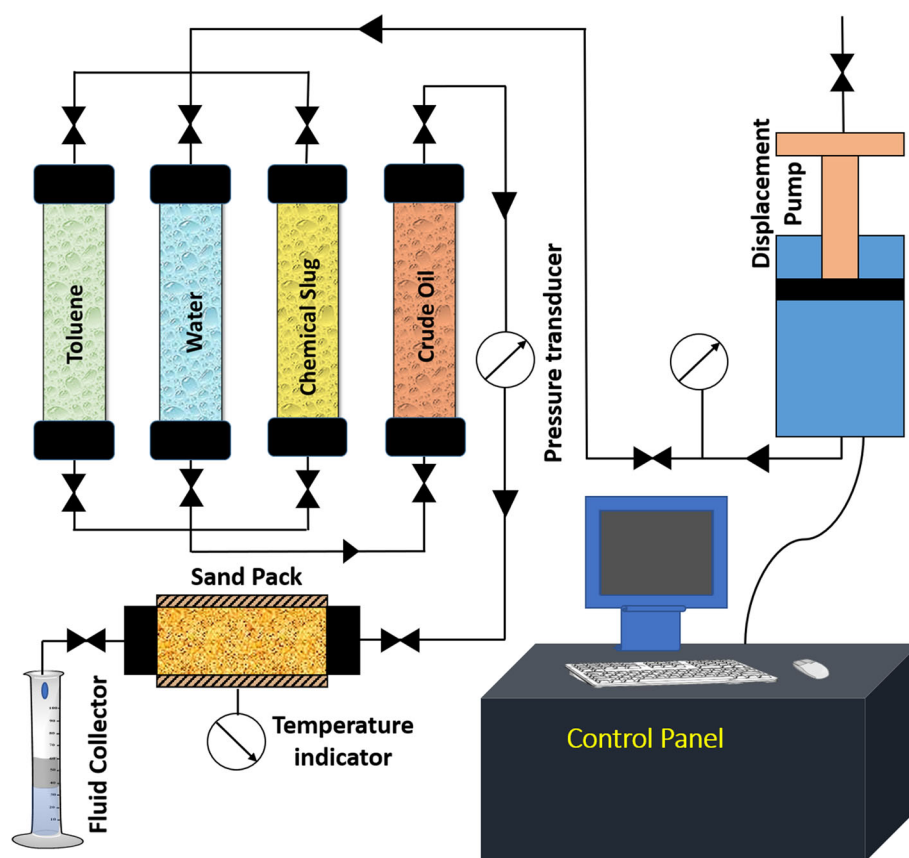
M_s is mass of solution in grams.

M_r is mass of adsorbent added in surfactant solution in grams.

3 Results and Discussion

3.1 Critical Micelle Concentration (CMC) Measurement

CMC is one of the most crucial parameters while injection of surfactant during CEOR. CMC can be described as the lim-

Fig. 2 Schematic of the sand pack flooding apparatus

iting concentration of the surfactant molecules above which they start to form micelles. Several methods can be used to obtain the CMC of the surfactant such as UV spectroscopy, surface tension, pH and conductivity measurement [37]. In present work, the CMC value of surfactant was explored by measuring the conductivity and surface tension values. The addition of surfactant reduces the surface tension value due to the adsorption of the surfactant particles at the liquid–air interface. However, surface tension does not reduce after a certain concentration of surfactant in the system which is described as the CMC of the surfactant (Fig. S3a). It can be explained as the particles of surfactant start to form micelles above CMC, which does not adsorb at the liquid–air interface leading to insignificant variation in the values of surface tension after attaining CMC [38]. The surface tension value of deionized water used in the experiment was found to be 72.4 mN/m which reduces to value of 34.5 mN/m with the addition of 2500 ppm of surfactant in the water at a temperature of 30 °C.

Conductivity method is based on the number of the ions present in the system that are responsible for the flow electrons through the system. The surfactant upon mixing in the water dissociates into cation and anion which gives rise to the conductivity of sample with surfactant concentration in the water (Fig. S3b). The rate of rise of conductivity changes sig-

nificantly at a certain concentration that is defined as the CMC of the surfactant [36]. This change in the slope arises because of micellization of free surfactant particles present in the system due to which ions present in the system do not increase leading to lower slope of conductivity versus concentration plot after CMC. The turning point of the plot was obtained at 2464 ppm, which is known as CMC of the surfactant at the temperature of 30 °C. Both the methods (conductivity as well as surface tension) gave the CMC approximately 2500 ppm, corroborating each other. Also, approximate value of the CMC (6.8 mmol/L-9.68 mmol/L) of surfactant (SDS) was obtained in the previous works [39, 40].

3.1.1 Effect of Temperature on CMC of the Surfactant

Subsurface temperature is always higher than the surface temperature which makes it imperative to explore the impact of temperature on the micellization behavior of the surfactant. The surfactant's CMC was revealed to rise at higher temperature. It increased from 2500 to 2700 ppm as the temperature rose from 30 to 75 °C, respectively (Fig. S4a). This could be explained by the amplified repulsive force experienced by the likely charged surfactant monomers at higher temperature due to increase in their kinetic energy. At an elevated temperature, the particles start to collide with the other

particles leading to higher electrostatic repulsion between the like-charged particles resulting in delay in the micellization of the surfactant and hence higher CMC values were obtained at higher temperatures. Another possible explanation could be the increase in the adsorption of the surfactant monomers at the airliquid interface at higher temperature due to higher entropy of the system [41]. This makes adsorption of particles more closely at the interface hence, higher CMC values are observed. These findings corroborate with a previous study [41, 42].

3.1.2 Effect of Concentration of NPs on CMC of the Surfactant

Addition of NPs in the surfactant solution was found to affect the surfactant's CMC. The value of CMC was reduced steeply with the addition of NPs in the surfactant solution. The surfactant's CMC turned down from 2500 to 2300 ppm, 2000 ppm and 1900 ppm upon addition of 100 ppm, 500 ppm and 1000 ppm of NPs (Fig. S4b). The fall in the CMC value can be explained by the increment in solution's ionic strength with the addition of NPs in it [43, 44]. The NPs being smaller in size would have greater surface area as well as higher surface free energy, this would lead to the dissociation of the ions that would reduce the electrostatic repulsion amongst the likely charged head group of the surfactant particles [15, 45]. This would encourage formation of micelles in the surfactant even at lower concentration leading to the decrease in the CMC value with NPs addition [46, 47]. Similar trend of the CMC value with NPs addition was obtained in an earlier work [15].

3.1.3 Comparison Between the CMC Values Obtained from Conductivity Method and Surface Tension Method

The CMC values obtained from both methods were approximately the same. Since, surface tension measurement method for CMC determination depends on the concentration of the surfactant solution made. The minimum value of the surface tension obtained at the surfactant concentration gives the value of its CMC. The surfactant solution of various concentration was of multiple 100 ppm, therefore CMC obtained using surface tension measurement was always in 100 ppm multiple whereas for conductivity method, the CMC was obtained from the intersection point of the two straight line using curve fitting. Hence, all the CMC values obtained using conductivity method were distinct. However, both the methods gave approximately the same CMC values suggested that both methods can be used to obtain the value of the surfactant's CMC.
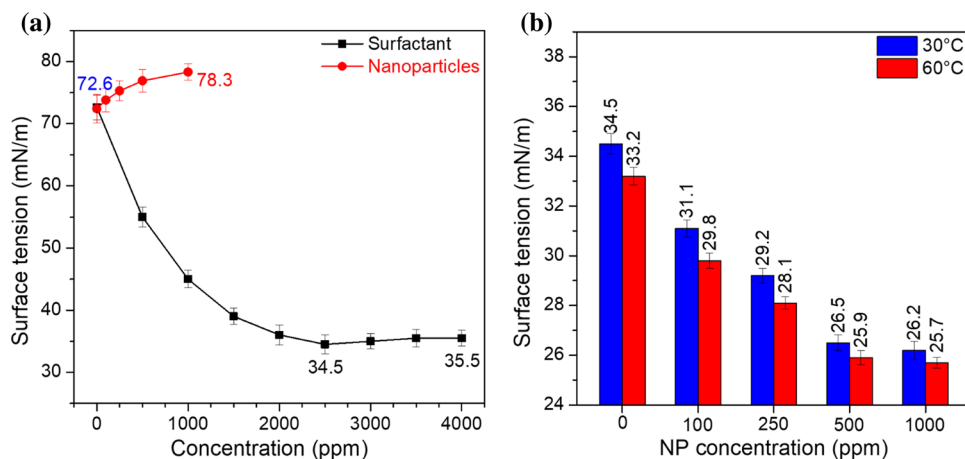
3.2 Surface Tension

The surface tension value was showing a reducing trend with increasing concentration of surfactant in the solution. However, surfactants have a tendency to form micelles in the solution after a particular concentration is identified as the CMC of the surfactant. Surface tension of the deionized water was found to be 72.4–72.6 mN/m at 30 °C, which reduced drastically upon introduction of surfactant. However, the surface tension values did not change significantly after the CMC value of the surfactant. This phenomenon can be explained by the adsorption of the surface-active agent's monomers at the air–liquid interface resulted in balancing the forces acting at the surface [4, 48]. As the surfactant concentration was increased further, the interface got saturated with the surfactant particles and it began to form micelles which did not reduce the surface tension [49]. The minimum surface tension value obtained with the surfactant was 34.5 mN/m at 2500 ppm and 30 °C. A slight increase in surface tension value at 4000 ppm of solution can be due to the desorption of surfactant particles from the interface. Previous studies corroborate the present findings [50, 51]. Unlike surfactant, NPs are not amphiphile but are completely hydrophilic in nature and also are positively charged. They do not have a tendency to get adsorbed at the air–liquid interface. However, NPs hydration is possible in an aqueous solution making it even harder to get adsorbed at the interface to reduce the surface tension [52]. Hence, an increase in the surface tension value was obtained with the NPs addition in the water (Fig. 3a). However, the increment in the surface tension value was not as steep as it was for surfactant solution. The surface tension value of the deionized water increased from 72.6 to 78.3 mN/m upon the addition of 1000 ppm of NPs in the water at 30 °C.

3.3 Synergistic effect of NPs concentration with surfactant solution on the surface tension

The addition of a smaller concentration of NPs with surfactant solution is known to reduce the surface tension. However, at higher concentration, it migrates the surfactant particles from the bulk phase [53], because of which NPs addition with surfactant solution of 2500 ppm was explored only up to 1000 ppm of NPs. The surface tension of the mixture of NPs and surfactants was obtained to be more efficient in reducing the surface tension as compared to that of the surfactant solution only. Surface tension reduced from 34.5 mN/m to 31.1 and further up to 26.2 upon addition of 100 ppm and 1000 ppm of NPs with 2500 ppm solution of surfactant at a temperature of 30 °C (Fig. 3b). This could be justified by the decrease in electrostatic interaction among the like-charged particles which are dispersed in water (surfactant and NPs). Positively charged NPs particles dispersed in the

Fig. 3 Surface tension measurement: (**a**) effect of concentration of surfactant and NPs individually on the surface tension of the deionized water; (**b**) synergistic effect of surfactant (2500 ppm) and NPs on the surface tension of the deionized water at different temperatures

water reduce the repulsion among the surfactant molecules of the same charged and vice versa [52]. This results in higher adsorption of the surfactant particles at the interface leading to lower surface tension values. An increase in temperature also had a positive effect on the minimization of the value of surface tension. The surface tension of 2500 ppm surfactant and 500 ppm NPs reduced from 26.5 mN/m to 25.9 mN/m with rise in temperature from 30 to 60 °C, respectively. This might be because of the increase in the kinetic energy of the particles dispersed in the aqueous solution which causes higher adsorption of the particles at the interface leading to lower surface tension values at higher temperatures [54]. Another possible explanation for the same could be an increase in particle's tendency to evaporate at higher temperatures resulting in higher adsorption at the interface [52]. The synergistic effect of the NPs addition with the surfactant on the surface tension is in agreement with the previous literature [55–59].

3.4 Interfacial Tension

IFT arises because of the disparity in the forces present between the interface of the two immiscible fluids [60, 61]. Injection fluid (chase water) and reservoir fluid have a large difference in their surface acting forces which are balanced by the injection of a chemical slug that could be a combination of various additives such as surfactant, polymer, alkali and nanoparticles. The selection of surfactant type is generally based on the type of reservoir. The present study focuses on the sand formation which are negatively charged and hence the most suitable surfactant type used for negatively charged reservoir rock is anionic surfactant due to the fact that Coulombic interaction would lead to the minimum loss of surfactant. Hence, the surface tension and wettability studies were done only with the combination of surfactant and nanoparticles. The addition of surfactant is known to cause a reduction in the IFT between the water and oil phases [50].
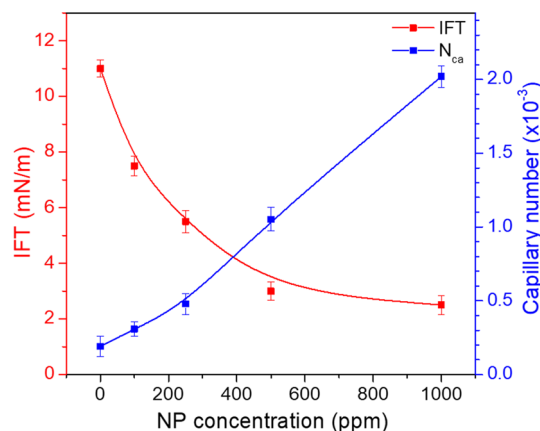

Fig. 4 Synergistic effect of NPs and fixed surfactant solution on the IFT and capillary number between the crude oil and mixed solution of surfactant and NPs of varying concentration

The effect of the addition of bio-Ca NPs with the surfactant solution of a fixed concentration (2500 ppm) on the IFT was studied at the atmospheric pressure and 30 °C. NPs addition had a positive impact on the minimization of IFT. The values reduced from 11.2 mN/m to a minimum value of 2.5 mN/m upon the addition of 1000 ppm NPs with 2500 ppm surfactant solution (Fig. 4). IFT minimization could be because of the electrostatic interaction between the head groups of the surfactant that are negatively charged and the positively charged NPs particle [52]. This could give rise to the surfactant particles getting adsorbed at the liquid interface at a higher rate due to lesser repulsion between the surfactant particles leading to reduced IFT values. However, this reduction was not significant when the concentration of the NPs was higher. This could be explained by the agglomeration of the NPs at higher concentrations leading to settling down of the NPs due to increased size. IFT measurement at 60 °C were also taken at given in Fig. S5.

Furthermore, reduction in IFT leads to an increase in the capillary number (ratio of the capillary and viscous forces)

which is known to have a direct impact on the oil recovery factor. It is obtained using Eq. 2 where N_{ca} is the capillary number; μ_w is the injection fluid viscosity; v is the injection fluid velocity; σ_{ow} is the IFT between the injection and displaced fluid [62]. Lower IFT reduces the capillary pressure performing at the oil drops residing at the smaller pores, making it simpler to mobilize the oil with injection fluid from the smaller pores [63]. Lower capillary pressure also means a higher capillary number. It can be inferred from the capillary number data (Eq. 2) that a better oil recovery factor could be achieved corresponding to the chemical slug having the lowest IFT value.

$$N_{ca} = \mu_w v / \sigma_{ow} \tag{2}$$

3.5 Contact Angle Studies

Wettability analysis of a surface was examined by determining the values of contact angle. The impact on the surface wettability of the sand pellet was studied over a wide range of surfactant concentrations. The contact angle was found to be inversely proportional to the surfactant concentration (Fig. 5a). The contact angle value of deionized water on the oil-wet surface was found to be 126° which minimized up to 30° upon the addition of 4000 ppm of surfactant in it. The reduction in the value of contact angle could be explained by the loss of surfactant due to its adsorption on the solid oil-wet pellet surface [49, 64]. The tail of the surfactant is hydrophobic in nature and interacts with the non-polar portion of the crude oil (carboxylate group) thereby forming a hydrophobic bond that gives rise to the adsorption of surfactant particles on the oil-wet solid surface exposing the hydrophilic charged group making the surface water wet. Modification in wettability of the surface can lead to the distortion of the oil film adsorbed at the solid surface [65]. This can form a mobile oil bank which could contribute to additional oil recovery. It is interesting to note that the reduction of the contact angle was drastic when surfactant concentration was added in a smaller amount. However, when the concentration of surfactant reaches beyond the CMC value, the difference in the contact angle values was found to be insignificant. This can be explained by the saturation of the solid surface with the adsorbed surfactant. The contact angle for each case was found to reduce after 600 s which can be attributed to the higher adsorption of the surfactant molecules corresponding to the higher exposure time. Adsorption is a time-dependent process and its value was found to be increasing with an increase in contact time which led to lower contact angles. The results obtained in the previous studies corroborate the present findings [59, 66]. Moreover, the experiment was also performed at 60 °C (Fig. S6).

A similar shift in the contact angle values was obtained upon the introduction of NPs with the deionized water suggesting the capability of the NPs to modify the wetting behavior of the oil-wet sand pellet. NPs because of their smaller size have a large surface free energy and have a greater tendency to get adsorbed on the surface. With an increase in the NPs concentration, lower contact angle values were obtained. This can be explained by the structural disjoining pressure which is a function of the NPs concentration in the solution [32, 67]. Disjoining pressure is the difference between the pressure at the bulk phase and the pressure at the wedge film. Higher NPs concentration would result in the higher accumulation of the NPs at the wedge film resulting in exerting greater disjoining pressure and hence lower contact angle would be obtained [68]. Similar to the surfactant, an increase in contact time resulted in a lower contact angle.

NPs when combined with anionic surfactant gave better results. Lower contact angle values were obtained when 2500 ppm of surfactant solution was mixed with NPs of various concentrations (Fig. 5b). This can be described by the decrease in electrostatic repulsion present among the electronegative charged particles of the surfactant in the bulk phase upon introduction of the NPs. Since NPs provide counterion which reduces the repulsion between the surfactant particles leading to higher adsorption of the surfactant and NPs at the solid surface. The contact angle value decreases from 31° to 18° when 1000 ppm of NPs was mixed with 2500 ppm of surfactant solution. It can be inferred from the contact angle of the mixture of NPs and surfactant that the mixture alters the surface wettability towards strong water-wet from water wet which is preferential for the oil displacement from the pores.

The mechanism responsible for the alteration in wettability towards water-wet from oil-wet using the NPs and surfactant mixture is explained in Fig. 6. The NPs adsorption on the surface creates a wedge film which in turn applies the disjoining pressure on the oil drop [69]. The disjoining pressure if exceeds a certain limit, the crude oil drop is removed from the surface. At the same time, the concentration of the surfactant monomers also gets reduced due to its adsorption on the oil-wet surface because of the hydrophobic interaction creating the surface water wet. The combined effect of NPs and surfactant efficiently altered the oil-wet nature of the sand pellet towards strong water-wet which might be proved critical during the oil displacement process.

3.6 Viscometry Analysis

The fluid when injected in the sand column, having its own permeability and porosity, follows a tortuous path. Hence, it becomes imperative to determine the flow behavior of the injection chemical slug at a wider shear range. The addition of NPs with the SP slug affects the viscosity of the solution. The NP type, shape and size have a great impact on the viscosity

Fig. 5 Dynamic contact angle measurement on the oil-wet sand pellet: (**a**) surfactant and NPs solution individually; (**b**) NPs of varying concentration mixed with 2500 ppm of surfactant solution
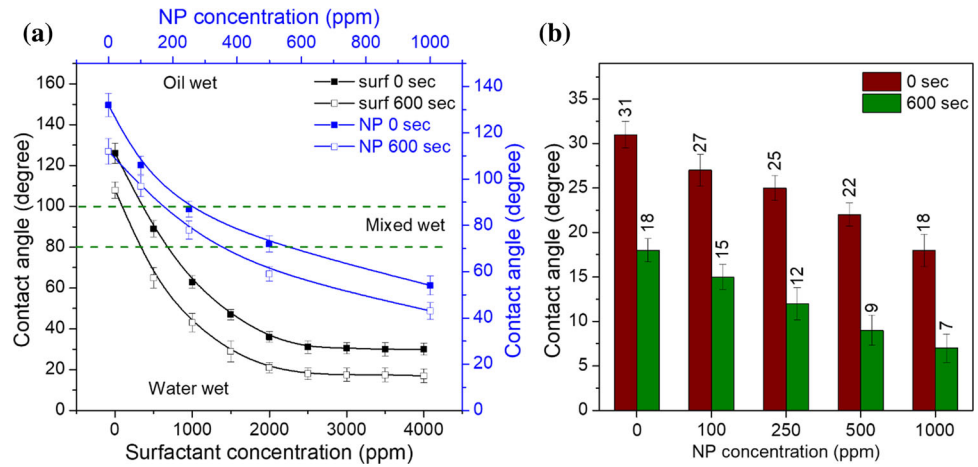

Fig. 6 Wettability alteration mechanism involved when NPs and surfactant are mixed in the chemical slug
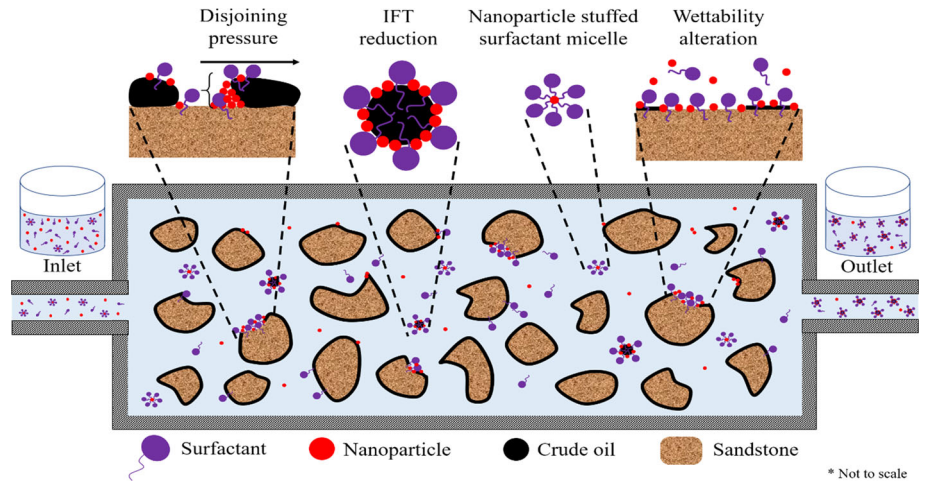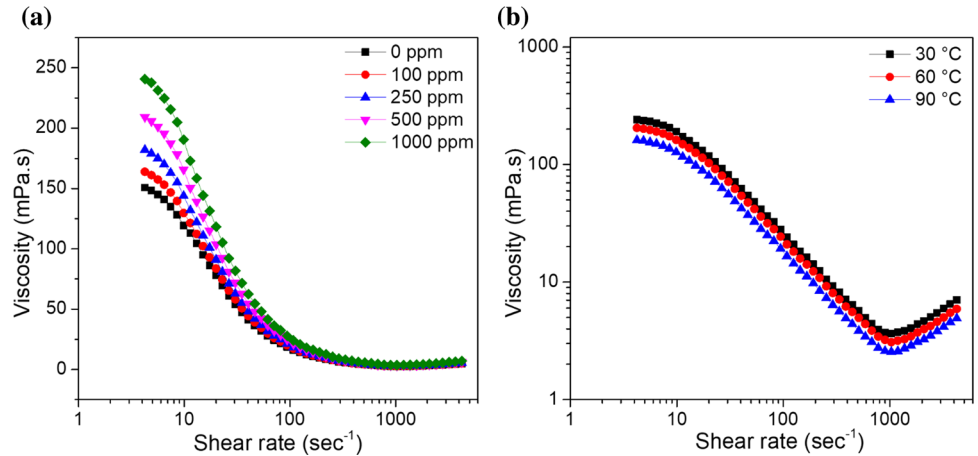

Fig. 7 Viscosity as function of shear rate: (**a**) effect of NPs concentration on SP slug (1000 ppm polymer and 2500 ppm surfactant) viscosity; (**b**) effect of temperature on the viscosity of 1000 ppm NPs mixed with SP slug

of the chemical slug [15]. The viscosity of the slug having a mixture of surfactant (2500 ppm), polymer (1000 ppm) and NPs with varying concentrations of NPswas examined with respect to shear rate. The concentration of polymer and surfactant was kept constant as the objective of the work was to explore the impact of NPs. The viscosity of the chemical slug at 20 s^{-1} shear rate and 30 °C was found to increase from

77.86 mPa.s to 83.72 mPa.s, 91.33 mPa.s, 103.74 mPa.s, and 118.26 mPa.s upon addition of 100, 250, 500 and 1000 ppm of NPs with the SP slug (Fig. 7a). The increment in the viscosity could be due to the presence of more solid particles in the slug that could have caused more friction between the long polymeric chain resulted in higher viscosity [70, 71]. The other likely elucidation for the same could be the devel-

opment of a complex structure between the NPs and polymer at the molecular level that could increase the viscosity values at higher NPs concentrations. The improvement in the viscosity values with NPs addition can be beneficial for the oil displacement, as higher injection fluid viscosity reduces the mobility ratio and could avoid viscous fingering of the fluid and provide better displacement efficiency [21].

Another interesting thing to observe is the reduction in the viscosity with the shear rate up to a certain value. The reduction in the viscosity can be interpreted as the shear-thinning property present in non-Newtonian fluids. The viscosity of a slug having 500 ppm NPs in the mixture of surfactant (2500 ppm) and polymer (1000 ppm) solution was found to be decreasing from 209.32 mPa.s to 103.74 mPa.s, 21.09 mPa.s and 3.24 mPa.s with the increase in shear rate from 4.24 to $20\ s^{-1}$, $108\ s^{-1}$ and $899\ s^{-1}$, respectively. The important point to note here is that the viscosity of the slug started to increase at a further higher shear rate. This can be explained by the order–disorder theory (ODT) [72]. The particles dispersed in the slug began to realign themselves from an ordered state to a disordered state resulting in higher viscosity values. Another possible explanation for the dilatant behavior of the chemical slug at a higher shear rate could be the formation of the hydroclusters (hydrodynamic lubrication theory) [73]. At a higher shear rate, the forces acting at the particles arranged in layered fashion exceeds, this destabilizes the particles' arrangement and results in higher particles interaction that gives rise to the viscosity at a higher shear rate. The viscosity of the chemical slug, formed by adding 1000 ppm NPs in the mixture of surfactant (2500 ppm) and polymer (1000 ppm), increases from 3.69 to 4.65 mPa.s and 7.03 mPa.s as the shear rate was increased from 899 to $2090 s^{-1}$ and $4240\ s^{-1}$ shear rate, respectively.

The slug (polymer 1000 ppm, surfactant 2500 ppm and NPs 1000 ppm) viscosity were also examined at various temperatures (30, 60 and 90 °C). A reducing trend in the viscosity of chemical slug was found at an elevated temperature. When the temperature of the slug was raised to 60 °C from 30 °C, its viscosity reduces to 204.58 mPa.s from 240.69 mPa.s and it reaches a value of 161.26 mPa.s when the temperature was further elevated to 90 °C (Fig. 7b). This reduction in the viscosity value can be described by the rupture in the large complex polymeric chain at higher temperatures leading to reduced viscosity values [49, 74]. The breakage of weak entanglement of the polymeric chain can be due to amplified kinetic energy of the particles at a higher temperature, as a result of which the viscosity of the chemical slug was reduced [15]. Previous work corroborates with the present findings [72].

3.7 Particle Size

The particle size of the NPs added as an additive in the chemical slug greatly affects the performance of the slug. It has been documented by the researchers that the shape and size of the NPs affect the forces present at the interface of the immiscible fluids as well as it also impacts the wettability alteration ability of the slug [75]. The average hydrodynamic diameter of the bio-Ca NPs used in the study was obtained to be 62 nm suspended in deionized water (Fig. 8). The pore throat plugging by NPs aggregation via mechanical trapping or log jamming can contribute to additional oil recovery by altering the wettability [18]. NP due to its smaller size has a great tendency to form an agglomerate. NPs can block the path of least resistance because of agglomeration of NPs at the pore throats, forcing the slug to flow through the oil-filled trapped. This would alter the wettability of the zone and recover the trapped oil by disjoining pressure mechanism. Another advantage that can enhance the performance of the conventional SP flooding via NP addition is the balancing of the interfacial forces between the oil and injection fluid. NPs have a great tendency to get adsorbed on the interface of the fluid because of their large surface energy [21, 75]. Being smaller in size, NP can intrude through the pore throats that might contain trapped left-out oil. NPs can adsorb on the interface of the oil residing at the pore throats and injection fluid leading to the reduction of the IFT and lowering of the capillary pressure [15]. This was evident in the IFT measurement where the addition of NP showed a synergistic effect of the IFT minimization because of less electrostatic repulsion present between the surfactant monomers due to the counterion produced by the NPs. This could cause the left out to flow from the pore throats and contribute to the additional oil recovery. Also, being positively charged, these bio-Ca NPs could keep the negatively charged surfactant monomers in the bulk phase, thereby reducing the loss of surfactant on the surface of rocks due to its adsorption. The positive impact of the NPs addition with the chemical slug was also observed in the viscometry analysis. The combined effect of the wettability alteration, pore plugging, IFT minimization and improved viscosity of the slug should have a positive impact on the oil displacement studies.

3.8 Sand Pack Flooding Results

Oil displacement of the SP slug blended with the bio-Ca NPs was studied by carrying out the sand pack flooding experiment. The sand column was prepared by ramming the cleaned and sorted sand particles of 250–400 microns into the sand column holder. The permeability of the sand column was evaluated with the help of Darcy's law. The primary and secondary recovery process were simulated by injecting water into the sand pack. Oil recovery of 47–49% was obtained for
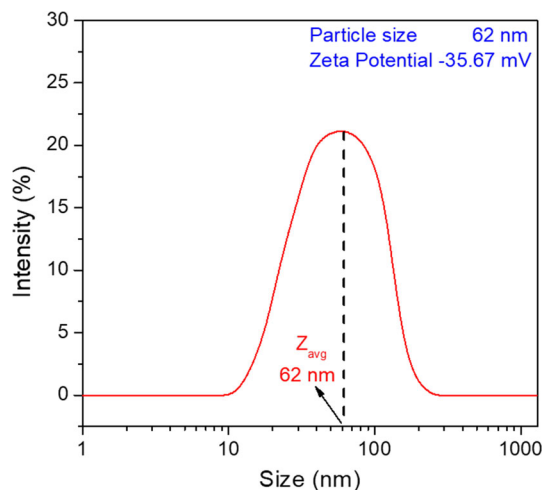
Fig. 8 Particle size and zeta potential of the bio-Ca NPs used for the experiment

every case during water flooding. SP chemical slug mixed with the NPs was injected in the sand column after water flooding to investigate its potential to mobilize the left-out oil from the reservoir pores. Additional oil recovery of 21.14% was obtained corresponding to the conventional SP chemical slug with no NPs mixed with the slug. However, as the NPs were mixed with the chemical slug, an increase in additional oil recovery was observed. The additional oil recovery of 23.86, 25.45, 27.19 and 27.71% was noted corresponding to 100, 250, 500 and 1000 ppm of NPs added with the mixture of 2500 ppm surfactant and 1000 ppm polymer solution (Fig. 9a). Higher oil recovery could be attributed to the lower IFT values (Sect. 3.3) and wettability alteration (Sect. 3.4) which was evident in the previous section. Injection of the chemical slug with NPs was found to be efficient to modify the wetting characteristic of the rock towards strong water-wet from oil-wet. This could possibly remove the adsorbed oil layer from the sand surface, which could contribute to the mobile oil phase giving rise to the total oil recovery factor. Furthermore, injection of the chemical slug can block the water channel, diverting the flow towards the oil trapped zone. This could possibly displace the trapped oil from the smaller pores contributing to additional oil recovery.

The production phase from a well not only involves oil recovery but simultaneously water production as well. The water cut was monitored throughout the flooding experiment. A characteristic curve obtained with the water cut as a function of injection volume was presented in Fig. 9b. Water cut results of all the flooding experiment was found to be similar. However, it was found that the water cut suddenly decreased around 2 PV. During the drop of water cut, an increase in the oil recovery at the production end was evident results. It is interesting to note that the chemical slug injection was from 1.5 to 2.0 PV whereas the decrease in the value of water cut
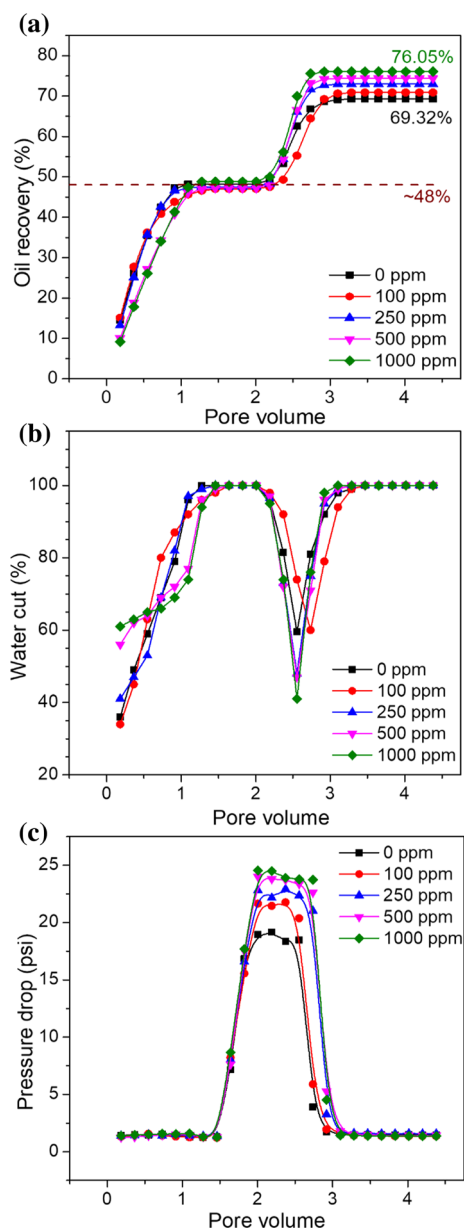

Fig. 9 Sand pack flooding experiment: (**a**) oil recovery results; (**b**) water cut results; (**c**) pressure drop results

was noted around 2PV. This could be possible because the chemical slug fluid front takes some time to flow towards the production end from the injection point. Ahead of the chemical slug, a mobile bank would have formed which upon production reduced the water cut drastically. Another important point to mention here is that the water cut didn't start from 0, this could be explained by the presence of the immobile water in the sand pack that would have become mobile upon water injection.

An equally important parameter worth studying is the pressure drop which can be described as the pressure difference across both the ends of the sand column. Pressure drop

Table 3 Various flooding parameters obtained while oil displacement studies

Run No	Slug composition	Φ (%)	Recovery Factor (%)			Saturation (%)		
			Secondary	Tertiary	Total	S_{wi}	S_{oi}	S_{or}
1	SP slug + 0 ppm NP	35.51	48.18	21.14	69.32	19.71	80.29	30.68
2	SP slug + 100 ppm NP	35.11	47.02	23.86	70.88	19.56	80.44	29.12
3	SP slug + 250 ppm NP	36.15	47.53	25.45	72.98	20.07	79.93	27.02
4	SP slug + 500 ppm NP	34.85	47.23	27.19	74.42	19.33	80.67	25.58
5	SP slug + 1000 ppm NP	34.59	48.34	27.71	76.05	20.22	79.78	23.94

gives an indication about the pumping pressure required during the injection of the water, chemical slug or chase water during the production phase from the reservoir. A pressure drop of ~ 1.25–1.51 psi was observed during the water flooding. However, it was observed that there was a sudden rise in the injection pressure at 1.5 PV that could be explained by the change in the injection fluid. From 0 to 1.5 PV, the injection fluid was water having viscosity of ~ 0.46 mPa.s at a temperature of 60 °C whereas from 1.5 to 2.0 PV, the injection fluid was a chemical slug having significantly higher viscosity as compared to that of water. This would have caused an increase in the pressure drop values. It is worth mentioning here that the pressure drop values kept increasing till 2.0 PV because the injection fluid was kept injecting till 2.0 PV (Fig. 9c). After which, injection pressure values started to reduce gradually. This could also be explained by the change in injection fluid viscosity. The gradual decrease in the injection pressure could be attributed to the building of an oil bank in front of the chemical slug fluid front. Furthermore, a sudden fall in the pressure value indicates the breakthrough of the chase water through the sand column. This suggested that a channel has been formed inside the sand pack and no further oil could be produced from the sand column. Another important point worth mentioning here is that there is the larger area under the pressure drop curve corresponding to the larger oil recovery case. This could be explained by the formation of a larger oil bank in front of the slug causing more drag. Hence, higher injection pressure was required to push the fluid [35]. Various parameters evaluated during the flooding experiment are tabulated in Table 3.

3.8.1 Permeability Reduction Studies

The injection of a chemical slug inside the formation can sometimes reduce the formation permeability leading to formation damage. Hence, it is crucial to determine the degree of permeability reduction after the slug injection. The reduction in formation original permeability was determined after the slug was pumped inside the sand pack and water was fur-

ther as a pushing fluid until a steady-state flow was achieved. Darcy law was then used to determine the formation permeability and it was found to be 543 mD corresponding to the slug composed of 1000 ppm polymer, 2500 surfactant and 100 ppm nanoparticles. It is worth mentioning that the increase in the concentration of nanoparticles in the slug further leads to the reduction of formation permeability (Table 4). This could be attributed to the adsorption of agglomerated nanoparticles on the sand particles and smaller pore channels leading to the blockage of the flow path. Hence, a reduction in permeability was observed. This was further validated by the FESEM characterization of the sand particles and the EDX mapping (Fig. S7), which depicts the adsorption of nanoparticles on the sand surface. This could be the reason for the abbreviation in formation permeability.

3.9 Adsorption Studies

Losing surfactant on the surface of rock due to adsorption remains the major issue encountered with the surfactant injection. Adsorption of the surfactant on the surface of the rock is not preferable after a certain limit as it decreases the efficiency of surfactant to reduce IFT and hence, more amount of surfactant would be required to achieve the same results. A lot of factors can be responsible for the loss of surfactant such as hydrogen bonding, ion exchange, polar interaction, Van der Waal attraction forces, electrostatic interaction, chemical interaction etc. [76–80]. However, for anionic surfactant adsorption on negatively charged sand particles, the electrostatic force of repulsion acting among the likely charged surfactant monomers remains the primary reason for its adsorption. The amount of surfactant loss was evaluated with the comparison of the initial and final concentrations of surfactant present in the solution. Since surfactant adsorption is influenced by the amount of surface-active agent available in the system which increases with surfactant concentration. Hence, surfactant loss was found to increase with surfactant concentration as well. Although a plateau region was found above the CMC value of the

Table 4 Permeability reduction studies

S. No	Nanoparticle's concentration in slug (ppm)	Original permeability before slug injection (mD)	Reduced permeability after slug injection (mD)	Percentage reduction in permeability (%)
1	100	608	543	11
1	250	649	562	13
1	500	523	439	16
1	1000	567	454	20

Fig. 10 Adsorption studies of the surfactant on the sand particles: (**a**) impact of NPs concentration on the adsorption reduction; (**b**) NPs efficiency to reduce the surfactant adsorption
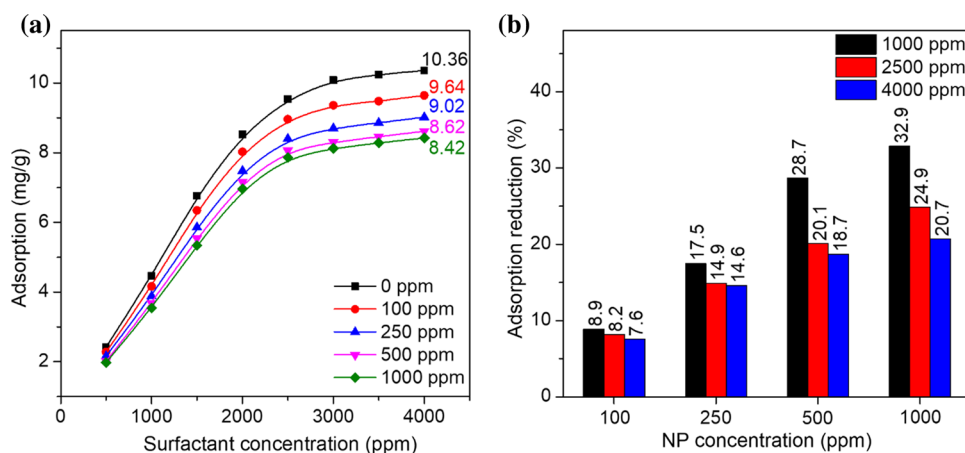
surfactant which can be described by micelle formation of surfactant monomers leading to fix the number of free surfactant particles present in solution [36, 37]. Hence, insignificant variation in the surfactant adsorption was obtained after the CMC value. Surfactant loss was found to increase from 2.42 to 9.54 mg/g and 10.36 mg/g as the surfactant concentration increases from 500 to 2500 ppm and 4000 ppm, respectively (Fig. 10a). Previous studies have reported similar findings [37, 81].

NPs addition for the surfactant adsorption reduction is not new [82, 83]. As the NPs were mixed with the surfactant solution, a reduction in the surfactant loss was observed. The surfactant loss was reduced for 4000 ppm of surfactant solution from 10.36 mg/g to 9.64 mg/g, 9.02 mg/g, 8.62 mg/g and 8.42 mg/g with the rise in the concentration of NPs in the system from 0 to 100, 250, 500 and 1000 ppm, respectively. The reduction in the surfactant loss with NPs addition could be attributed to the counterion produced by the NPs in the solution. The positively charged calcium ion produced from the dissociation of NPs in the aqueous solution interacts with the negatively charged surfactant head group. This leads to a decrease in the electrostatic repulsion in the similarly charged surfactant monomers resulting in lower adsorption values. This was also perceptible in the measurement of surface tension where counter ion produced by the NPs resulted in lower surface tension values. Another possible explanation for the same could be the interaction between the NP and surfactant molecules keeps most of the surfactant particles in the liquid phase, which restrict them to interact with the solid surface

[15, 82]. This also lowers the surfactant loss. The addition of NPs could also result in occupying the surface area accessible for the adsorption of the surfactant particles, causing a reduction in the area left for the surfactant particles to interact [84]. Competitive adsorption of NPs also reduces the surfactant interaction with the solid surface. This was also noted during the investigation of contact angle where adsorption of NPs shifts the wettability from oil-wet to strongly water-wet. Furthermore, being positively charged, NPs would interact with the sand surface more strongly as compared to that of the surfactant molecules. These interactions could lead to a decrease in the loss of surfactant because of its adsorption on the sand surfaces.

The tendency of NPs to decrease the surfactant's adsorption on the rock surface was seen to be larger corresponding to a larger concentration of NPs mixed with the surfactant solution. The adsorption of 1000 ppm surfactant solution was reduced from 8.9 to 32.9% as the NPs concentration was raised from 100 to 1000 ppm whereas the same for 2500 ppm of surfactant solution was found to 8.2% and 24.9%, respectively (Fig. 10b). An increase in NP concentration, increased the efficiency to reduce the surfactant adsorption. However, at higher surfactant concentrations lesser reduction in surfactant loss was observed. Adsorption reduction percentage for 500 ppm of NPs addition was found to be 28.7%, 20.1% and 18.7% corresponding to 1000 ppm, 2500 ppm and 4000 ppm of surfactant solution. This could be accredited to the rise in the ratio of the number of surfactant particles to the NPs concentration. A larger ratio means a greater num-

Table 5 Different adsorption isotherm fitted using adsorption data

NPs concentration (ppm)	Langmuir			Freundlich			Temkin		
	R^2	Q_o	K_{ad}	R^2	n	K_f	R^2	B	K_i
0	0.9928	27.93296	0.000192	0.9529	1.384083	0.030502	0.9756	4.1936	0.003411
100	0.9921	25.44529	0.000199	0.9497	1.395479	0.029819	0.9722	3.8834	0.003463
250	0.9927	22.72727	0.000211	0.9522	1.404103	0.028787	0.9719	3.6218	0.003468
500	0.9926	22.88303	0.000195	0.9514	1.383892	0.025328	0.9705	3.4868	0.003408
1000	0.9929	21.88184	0.000201	0.9542	1.378931	0.024161	0.9697	3.4209	0.003363

ber of surfactant particles would possibly interact with the solid surface and hence lower adsorption reduction efficiency was observed. Adsorption studies at flooding temperature were also conducted and the results are presented in supporting information (Fig. S8). The adsorption values were further fitted with the adsorption isotherm model (Langmuir, Freundlich and Temkin) [35]. The fitting and adsorption parameters are tabulated in Table 5.

4 Conclusions

Bio-Ca NPs showed a promising impact on the efficacy of the SP flooding technique. NPs effectively reduced the CMC of surfactant from 2500 to 1900 ppm with a mere 1000 ppm of NP addition. It can be inferred from the 24% reduction in the CMC value that a less amount of surfactant would be required for the process. Furthermore, IFT and wettability studies suggested that synergy exists between positively charged NPs and negatively charged surfactant particles. Strong water wetting characteristics and lower IFT with surfactant and NPs combined solution resulted in cumulative oil recovery of ~76% compared to ~69% with no NPs dispersed in the system. The addition of 1000 ppm of NPs reduced the surfactant adsorption by 33% and 25% of 1000 ppm and 2500 ppm surfactant solution, respectively. It can be deduced from the experimental results that the bio-Ca NPs have the potential to be used as an additive for the SP flooding technique to improve its efficiency to recover the residual oil. However, problem of agglomeration of nanoparticles needs to be tackled. Moreover, further studies on effect of bio-Ca nanoparticles on the rheology of the slug along with the extensive study on economic estimation are required to be explored, which can be done in future work before assessing its performance for field scale.

References

1. Nwidee, L.N.; Theophilus, S.; Barifcani, A.; Sarmadivaleh, M.; Iglauer, S.: EOR processes, opportunities and technological advancements. Chem. Enhanced Oil Recov. (cEOR) Prac. Overv. **1**, 3–52 (2016)

2. Gbadamosi, A.O.; Junin, R.; Manan, M.A.; Yekeen, N.; Augustine, A.: Hybrid suspension of polymer and nanoparticles for enhanced oil recovery. Polym. Bull. **76**(12), 6193–6230 (2019). https://doi.org/10.1007/s00289-019-02713-2

3. Sheng, J. J.: Surfactant-Polymer Flooding. Enhan. Oil Recov. Field Case Stud. 117–142 (2013)

4. Wu, Z.; Yue, X.; Cheng, T.; Yu, J.; Yang, H.: Effect of viscosity and interfacial tension of surfactant-polymer flooding on oil recovery in high-temperature and high-salinity reservoirs. J. Pet. Explor. Prod. Technol. **4**(1), 9–16 (2014). https://doi.org/10.1007/s13202-013-0078-6

5. Al-Anssari, S.; Barifcani, A.; Wang, S.; Maxim, L.; Iglauer, S.: Wettability alteration of oil-wet carbonate by silica nanofluid. J. Coll. Interface Sci. **461**, 435–442 (2016). https://doi.org/10.1016/j.jcis.2015.09.051

6. Aminnaji, M.; Fazeli, H.; Bahramian, A.; Gerami, S.; Ghojavand, H.: Wettability alteration of reservoir rocks from liquid wetting to gas wetting using nanofluid. Transp. Porous Media **109**(1), 201–216 (2015). https://doi.org/10.1007/s11242-015-0509-6

7. Hendraningrat, L.; Li, S.; Torsæter, O.: A coreflood investigation of nanofluid enhanced oil recovery. J. Pet. Sci. Eng. **111**, 128–138 (2013). https://doi.org/10.1016/j.petrol.2013.07.003

8. Soleimani, H., et al.: Synthesis of ZnO nanoparticles for oil–water interfacial tension reduction in enhanced oil recovery. Appl. Phys. A Mater. Sci. Process. (2018). https://doi.org/10.1007/s00339-017-1510-4

9. Cheraghian, G.; Hendraningrat, L.: A review on applications of nanotechnology in the enhanced oil recovery part B: effects of nanoparticles on flooding. Int. Nano Lett. **6**(1), 1–10 (2016). https://doi.org/10.1007/s40089-015-0170-7

10. Hendraningrat, L.; Torsæter, O.: Effects of the initial rock wettability on silica-based nanofluid-enhanced oil recovery processes at reservoir temperatures. Energy Fuels **28**(10), 6228–6241 (2014). https://doi.org/10.1021/ef5014049

11. Al-Anssari, S.; Barifcani, A.; Keshavarz, A.; Iglauer, S.: Impact of nanoparticles on the CO2-brine interfacial tension at high pressure and temperature. J. Coll. Interface Sci. **532**, 136–142 (2018). https://doi.org/10.1016/j.jcis.2018.07.115

12. Cheraghian, G.; Hendraningrat, L.: A review on applications of nanotechnology in the enhanced oil recovery part A: effects of nanoparticles on interfacial tension. Int. Nano Lett. **6**(2), 129–138 (2016). https://doi.org/10.1007/s40089-015-0173-4

13. Khalilinezhad, S.S.; Cheraghian, G.; Roayaei, E.; Tabatabaee, H.; Karambeigi, M.S.: "Improving heavy oil recovery in the polymer flooding process by utilizing hydrophilic silica nanoparticles.

Energy Sour. Part A Recover. Util. Environ. Eff. **00**(00), 1–10 (2017). https://doi.org/10.1080/15567036.2017.1302521

14. Cheraghian, G.: Effect of nano titanium dioxide on heavy oil recovery during polymer flooding. Pet. Sci. Technol. **34**(7), 633–641 (2016). https://doi.org/10.1080/10916466.2016.1156125

15. Kesarwani, H.; Sharma, S.; Mandal, A.: Application of novel colloidal silica nanoparticles in the reduction of adsorption of surfactant and improvement of oil recovery using surfactant polymer flooding. ACS Omega **6**(17), 11327–11339 (2021). https://doi.org/10.1021/acsomega.1c00296

16. Gbadamosi, A., Junin, R., Manan, M., Agi, A., Oseh, J.: Nanotechnology application in chemical enhanced oil recovery: current opinion and recent advances. In: Enhanced Oil Recovery Processes - New Technologies, (2019)

17. Kedir, A.S.; Seland, J.G.; Skauge, A.; Skauge, T.: Nanoparticles for enhanced oil recovery: influence of pH on aluminum-cross-linked partially hydrolyzed polyacrylamideinvestigation by rheology and NMR. Energy Fuels **28**(5), 2948–2958 (2014). https://doi.org/10.1021/ef5000694

18. Eltoum, H.; Yang, Y.L.; Hou, J.R.: The effect of nanoparticles on reservoir wettability alteration: a critical review. Pet. Sci. **18**(1), 136–153 (2021). https://doi.org/10.1007/s12182-020-00496-0

19. Yuan, L.; Zhang, Y.; Dehghanpour, H.: A theoretical explanation for wettability alteration by adding nanoparticles in oil-water-tight rock systems. Energy Fuels (2021). https://doi.org/10.1021/acs.energyfuels.1c00001

20. Giraldo, J.; Benjumea, P.; Lopera, S.; Cortés, F.B.; Ruiz, M.A.: Wettability alteration of sandstone cores by alumina-based nanofluids. Energy Fuels **27**(7), 3659–3665 (2013). https://doi.org/10.1021/ef4002956

21. Rezk, M.Y.; Allam, N.K.: Impact of nanotechnology on enhanced oil recovery: a mini-review. Ind. Eng. Chem. Res. **58**(36), 16287–16295 (2019). https://doi.org/10.1021/acs.iecr.9b03693

22. Hu, Z.; Azmi, S.M.; Raza, G.; Glover, P.W.J.; Wen, D.: Nanoparticle-assisted water-flooding in berea sandstones. Energy Fuels **30**(4), 2791–2804 (2016). https://doi.org/10.1021/acs.energyfuels.6b00051

23. Ju, B.; Fan, T.: Experimental study and mathematical model of nanoparticle transport in porous media. Powder Technol. **192**(2), 195–202 (2009). https://doi.org/10.1016/j.powtec.2008.12.017

24. Suleimanov, B.A.; Ismailov, F.S.; Veliyev, E.F.: Nanofluid for enhanced oil recovery. J. Pet. Sci. Eng. **78**(2), 431–437 (2011). https://doi.org/10.1016/j.petrol.2011.06.014

25. Esfandyari Bayat, A.; Junin, R.; Samsuri, A.; Piroozian, A.; Hokmabadi, M.: Impact of metal oxide nanoparticles on enhanced oil recovery from limestone media at several temperatures. Energy Fuels **28**(10), 6255–6266 (2014). https://doi.org/10.1021/ef5013616

26. Nazari Moghaddam, R.; Bahramian, A.; Fakhroueian, Z.; Karimi, A.; Arya, S.: Comparative study of using nanoparticles for enhanced oil recovery: wettability alteration of carbonate rocks. Energy Fuels **29**(4), 2111–2119 (2015). https://doi.org/10.1021/ef5024719

27. Islam, K.N., et al.: Facile synthesis of calcium carbonate nanoparticles from cockle shells. J. Nanomater. **2012**(1), 1–5 (2012). https://doi.org/10.1155/2012/534010

28. Islam, A.; Teo, S.H.; Rahman, M.A.; Taufiq-Yap, Y.H.: Seeded growth route to noble calcium carbonate nanocrystal. PLoS ONE **10**(12), 1–13 (2015). https://doi.org/10.1371/journal.pone.0144805

29. Qu, F.; Lin, H.; Wu, X.; Li, X.; Qiu, S.; Zhu, G.: Bio-templated synthesis of highly ordered macro-mesoporous silica material for sustained drug delivery. Solid State Sci. **12**(5), 851–856 (2010). https://doi.org/10.1016/j.solidstatesciences.2010.02.005

30. Jia, X.; Qian, W.; Wu, D.; Wei, D.; Xu, G.; Liu, X.: Cuttlebone-derived organic matrix as a scaffold for assembly of silver nanopar-

ticles and application of the composite films in surface-enhanced Raman scattering. Coll. Surf. B Biointerf. **68**(2), 231–237 (2009). https://doi.org/10.1016/j.colsurfb.2008.10.017

31. Ahmadi, R.; Osfouri, S.; Azin, R.: Wettability alteration of carbonate oil reservoir surface using biocompatible nanoparticles. Mater. Res. Expr. **6**(2), 25033 (2019). https://doi.org/10.1088/2053-1591/aaee57

32. Ahmadi, R.; Farmani, Z.; Osfouri, S.; Azin, R.: Condensate blockage remediation in a gas reservoir through wettability alteration using natural CaCO3 nanoparticles. Coll. Surf. A Physicochem. Eng. Asp. **579**, 123702 (2019). https://doi.org/10.1016/j.colsurfa.2019.123702

33. Gupta, A.; Pandey, A.; Kesarwani, H.; Sharma, S.; Saxena, A.: Automated determination of interfacial tension and contact angle using computer vision for oil field applications. J. Pet. Explor. Prod. Technol. (2021). https://doi.org/10.1007/s13202-021-01398-6

34. Daerr, A.; Mogne, A.: Pendent_Drop: an imagej plugin to measure the surface tension from an image of a pendent Drop. J. Open Res. Softw. **4**, 2–6 (2016). https://doi.org/10.5334/jors.97

35. Kesarwani, H.; Saxena, A.; Mandal, A.; Sharma, S.: Anionic/nonionic surfactant mixture for enhanced oil recovery through the investigation of adsorption, interfacial, rheological, and rock wetting characteristics. Energy Fuels **35**(4), 3065–3078 (2021). https://doi.org/10.1021/acs.energyfuels.0c03767

36. Ahmadi, M.A.; Sheng, J.: Performance improvement of ionic surfactant flooding in carbonate rock samples by use of nanoparticles. Pet. Sci. **13**(4), 725–736 (2016). https://doi.org/10.1007/s12182-016-0109-2

37. Ahmadi, M.A.; Shadizadeh, S.R.: Adsorption of novel nonionic surfactant and particles mixture in carbonates: enhanced oil recovery implication. Energy Fuels **26**(8), 4655–4663 (2012). https://doi.org/10.1021/ef300154h

38. Gao, B.; Sharma, M.M.: A family of alkyl sulfate gemini surfactants. 2. Water-oil interfacial tension reduction. J. Coll. Interface Sci. **407**, 375–381 (2013). https://doi.org/10.1016/j.jcis.2013.06.066

39. Wolowicz, A.; Staszak, K.: Study of surface properties of aqueous solutions of sodium dodecyl sulfate in the presence of hydrochloric acid and heavy metal ions. J. Mol. Liq. **299**, 112170 (2020). https://doi.org/10.1016/j.molliq.2019.112170

40. Marcolongo, J.P.; Mirenda, M.: Thermodynamics of sodium dodecyl sulfate (SDS) micellization: an undergraduate laboratory experiment. J. Chem. Educ. **88**(5), 629–633 (2011). https://doi.org/10.1021/ed900019u

41. Saxena, N.; Goswami, A.; Dhodapkar, P.K.; Nihalani, M.C.; Mandal, A.: Bio-based surfactant for enhanced oil recovery: interfacial properties, emulsification and rock-fluid interactions. J. Pet. Sci. Eng. **176**(5), 299–311 (2019). https://doi.org/10.1016/j.petrol.2019.01.052

42. Khoshnood, A.; Lukanov, B.; Firoozabadi, A.: Temperature effect on micelle formation: molecular thermodynamic model revisited. Langmuir **32**(9), 2175–2183 (2016). https://doi.org/10.1021/acs.langmuir.6b00039

43. Tanford, C.: The hydrophobic effect: formation of micelles and biological membranes (2nd Edition), 9(1) (1981)

44. Umlong, I.M.; Ismail, K.: Micellization of AOT in aqueous sodium chloride, sodium acetate, sodium propionate, and sodium butyrate media: a case of two different concentration regions of counterion binding. J. Coll. Interface Sci. **291**(2), 529–536 (2005). https://doi.org/10.1016/j.jcis.2005.05.003

45. Ahmadi, M.A.; Ahmad, Z.; Phung, L.T.K.; Kashiwao, T.; Bahadori, A.: Experimental investigation the effect of nanoparticles on micellization behavior of a surfactant: application to EOR. Pet. Sci. Technol. **34**(11–12), 1055–1061 (2016). https://doi.org/10.1080/10916466.2016.1148051

46. Eftekhari, M.; Schwarzenberger, K.; Javadi, A.; Eckert, K.: The influence of negatively charged silica nanoparticles on the surface properties of anionic surfactants: Electrostatic repulsion or the effect of ionic strength? Phys. Chem. Chem. Phys. **22**(4), 2238–2248 (2020). https://doi.org/10.1039/c9cp05475h

47. Palladino, P.; Ragone, R.: Ionic strength effects on the critical micellar concentration of ionic and nonionic surfactants: the binding model. Langmuir **27**(23), 14065–14070 (2011). https://doi.org/10.1021/la202897q

48. Bera, A.; Mandal, A.; Guha, B.B.: Synergistic effect of surfactant and salt mixture on interfacial tension reduction between crude oil and water in enhanced oil recovery. J. Chem. Eng. Data **59**(1), 89–96 (2014). https://doi.org/10.1021/je400850c

49. Kumar, S.; Saxena, N.; Mandal, A.: Synthesis and evaluation of physicochemical properties of anionic polymeric surfactant derived from Jatropha oil for application in enhanced oil recovery. J. Ind. Eng. Chem. **43**, 106–116 (2016). https://doi.org/10.1016/j.jiec.2016.07.055

50. Yuan, C.-D.; Pu, W.-F.; Wang, X.-C.; Sun, L.; Zhang, Y.-C.; Cheng, S.: Effects of interfacial tension, emulsification, and surfactant concentration on oil recovery in surfactant flooding process for high temperature and high salinity reservoirs. Energy Fuels **29**(10), 6165–6176 (2015). https://doi.org/10.1021/acs.energyfuels.5b01393

51. Babu, K.; Pal, N.; Bera, A.; Saxena, V.K.; Mandal, A.: Studies on interfacial tension and contact angle of synthesized surfactant and polymeric from castor oil for enhanced oil recovery. Appl. Surf. Sci. **353**, 1126–1136 (2015). https://doi.org/10.1016/j.apsusc.2015.06.196

52. Saien, J.; Rezvani Pour, A.; Asadabadi, S.: Interfacial tension of the n-hexane-water system under the influence of magnetite nanoparticles and sodium dodecyl sulfate assembly at different temperatures. J. Chem. Eng. Data **59**(6), 1835–1842 (2014). https://doi.org/10.1021/je401066j

53. Mohajeri, M.; Hemmati, M.: An experimental study on using a nanosurfactant in an EOR process of heavy oil in a fractured micromodel. J. Pet. Sci. Eng. **126**, 162–173 (2015). https://doi.org/10.1016/j.petrol.2014.11.012

54. Murshed, S.M.S.; Tan, S.H.; Nguyen, N.T.: Temperature dependence of interfacial properties and viscosity of nanofluids for droplet-based microfluidics. J. Phys. D. Appl. Phys. **41**(8), 1–5 (2008). https://doi.org/10.1088/0022-3727/41/8/085502

55. Saien, J.; Bahrami, M.: Understanding the effect of different size silica nanoparticles and SDS surfactant mixtures on interfacial tension of n-hexane–water. J. Mol. Liq. **224**, 158–164 (2016). https://doi.org/10.1016/j.molliq.2016.09.112

56. Pal, N.; Verma, A.; Ojha, K.; Mandal, A.: Nanoparticle-modified Gemini surfactant foams as efficient displacing fluids for enhanced oil recovery. J. Mol. Liq. **310**(14), 113193 (2020)

57. Kumar, A.; Mandal, A.: Critical investigation of zwitterionic surfactant for enhanced oil recovery from both sandstone and carbonate reservoirs: adsorption, wettability alteration and imbibition studies. Chem. Eng. Sci. **209**, 115222 (2019). https://doi.org/10.1016/j.ces.2019.115222

58. Pal, N.; Vajpayee, M.; Mandal, A.: Cationic/nonionic mixed surfactants as enhanced oil recovery fluids: influence of mixed micellization and polymer association on interfacial, rheological, and rock-wetting characteristics. Energy Fuels **33**(7), 6048–6059 (2019). https://doi.org/10.1021/acs.energyfuels.9b00671

59. Pillai, P.; Mandal, A.: A comprehensive micro scale study of polyionic liquid for application in enhanced oil recovery: synthesis, characterization and evaluation of physicochemical properties. J. Mol. Liq. **302**, 112553 (2020). https://doi.org/10.1016/j.molliq.2020.112553

60. Spaepen, F.: Homogeneous nucleation and the temperature dependence of the crystal-melt interfacial tension. Solid State Phys. Adv. Res. Appl. **47**, 1–32 (1994)

61. Berry, J.D.; Neeson, M.J.; Dagastine, R.R.; Chan, D.Y.C.; Tabor, R.F.: Measurement of surface and interfacial tension using pendant drop tensiometry. J. Coll. Interface Sci. **454**(18), 226–237 (2015). https://doi.org/10.1016/j.jcis.2015.05.012

62. Kesarwani, H.; Saxena, A.; Saxena, N.; Sharma, S.: Oil mobilization potential of a novel anionic karanj oil surfactant: interfacial, wetting characteristic, adsorption, and oil recovery studies. Energy Fuels **35**(13), 10597–10610 (2021). https://doi.org/10.1021/acs.energyfuels.1c01327

63. Ali, J.A.; Kolo, K.; Manshad, A.K.; Mohammadi, A.H.: Recent advances in application of nanotechnology in chemical enhanced oil recovery: effects of nanoparticles on wettability alteration, interfacial tension reduction, and flooding. Egypt. J. Pet. **27**(4), 1371–1383 (2018). https://doi.org/10.1016/j.ejpe.2018.09.006

64. Zdziennicka, A.; Jańczuk, B.: The relationship between the adhesion work, the wettability and composition of the surface layer in the systems polymer/aqueous solution of anionic surfactants and alcohol mixtures. Appl. Surf. Sci. **257**(3), 1034–1042 (2010). https://doi.org/10.1016/j.apsusc.2010.08.012

65. Putra, W.; Hakiki, F.: Microbial enhanced oil recovery: interfacial tension and biosurfactant-bacteria growth. J. Pet. Explor. Prod. Technol. **9**, 2353–2374 (2019). https://doi.org/10.1007/s13202-019-0635-8

66. Liu, J.; Sheng, J.J.; Wang, X.; Ge, H.; Yao, E.: Experimental study of wettability alteration and spontaneous imbibition in Chinese shale oil reservoirs using anionic and nonionic surfactants. J. Pet. Sci. Eng. **175**, 624–633 (2019). https://doi.org/10.1016/j.petrol.2019.01.003

67. Radnia, H.; Rashidi, A.; Solaimany Nazar, A.R.; Eskandari, M.M.; Jalilian, M.: A novel nanofluid based on sulfonated graphene for enhanced oil recovery. J. Mol. Liq. **271**, 795–806 (2018). https://doi.org/10.1016/j.molliq.2018.09.070

68. Li, S.; Torsæter, O.; Lau, H.C.; Hadia, N.J.; Stubbs, L.P.: The impact of nanoparticle adsorption on transport and wettability alteration in water-wet Berea sandstone: an experimental study. Front. Phys. (2019). https://doi.org/10.3389/fphy.2019.00074

69. Pogaku, R., et al.: Polymer flooding and its combinations with other chemical injection methods in enhanced oil recovery. Polym. Bull. **75**(4), 1753–1774 (2018). https://doi.org/10.1007/s00289-017-2106-z

70. Rezvani, H.; Riazi, M.; Tabaei, M.; Kazemzadeh, Y.; Sharifi, M.: Experimental investigation of interfacial properties in the EOR mechanisms by the novel synthesized Fe3O4@Chitosan nanocomposites. Coll. Surf. A Physicochem. Eng. Asp. **544**, 15–27 (2018). https://doi.org/10.1016/j.colsurfa.2018.02.012

71. Mahbubul, I.M.; Saidur, R.; Amalina, M.A.: Latest developments on the viscosity of nanofluids. Int. J. Heat Mass Transf. **55**(4), 874–885 (2012). https://doi.org/10.1016/j.ijheatmasstransfer.2011.10.021

72. Kumar, S.; Mandal, A.: Rheological properties and performance evaluation of synthesized anionic polymeric surfactant for its application in enhanced oil recovery. Polymer (Guildf) **120**, 30–42 (2017). https://doi.org/10.1016/j.polymer.2017.05.051

73. Maranzano, B.J.; Wagner, N.J.: The effects of particle size on reversible shear thickening of concentrated colloidal dispersions. J. Chem. Phys. **114**(23), 10514 (2001). https://doi.org/10.1063/1.1373687

74. Hashmet, M.R.; Onur, M.; Tan, I.M.: Empirical correlations for viscosity of polyacrylamide solutions with the effects of temperature and shear rate. II. J. Dispers. Sci. Technol. **35**(12), 1685–1690 (2014). https://doi.org/10.1080/01932691.2013.873866

75. Bhuiyan, M.H.U.; Saidur, R.; Amalina, M.A.; Mostafizur, R.M.; Islam, A.K.M.S.: Effect of nanoparticles concentration and their sizes on surface tension of nanofluids. Procedia Eng. **105**, 431–437 (2015). https://doi.org/10.1016/j.proeng.2015.05.030

76. Biswas, S.C.; Chattoraj, D.K.: Kinetics of adsorption of cationic surfactants at charcoal-water interface. J. Surf. Sci. Technol. **14**(1–4), 78–92 (1998). https://doi.org/10.18311/jsst/1998/2101

77. Mannhardt, K.; Schramm, L.L.; Novosad, J.J.: Adsorption of anionic and amphoteric foam-forming surfactants on different rock types. Coll. Surf. **68**(1–2), 37–53 (1992). https://doi.org/10.1016/0166-6622(92)80146-S

78. Azam, M.R.; Tan, I.M.; Ismail, L.; Mushtaq, M.; Nadeem, M.; Sagir, M.: Static adsorption of anionic surfactant onto crushed Berea sandstone. J. Pet. Explor. Prod. Technol. **3**(3), 195–201 (2013). https://doi.org/10.1007/s13202-013-0057-y

79. Saxena, N.; Kumar, A.; Mandal, A.: Adsorption analysis of natural anionic surfactant for enhanced oil recovery: the role of mineralogy, salinity, alkalinity and nanoparticles. J. Pet. Sci. Eng. **173**, 1264–1283 (2019). https://doi.org/10.1016/j.petrol.2018.11.002

80. Somasundaran, P.; Huang, L.: Adsorption/aggregation of surfactants and their mixtures at solid-liquid interfaces. Adv. Coll. Interface Sci. **88**(1–2), 179–208 (2000). https://doi.org/10.1016/S0001-8686(00)00044-0

81. Ahmadi, M.A.; Shadizadeh, S.R.: Induced effect of adding nano silica on adsorption of a natural surfactant onto sandstone rock: experimental and theoretical study. J. Pet. Sci. Eng. **112**, 239–247 (2013). https://doi.org/10.1016/j.petrol.2013.11.010

82. Yekeen, N.; Manan, M.A.; Idris, A.K.; Samin, A.M.; Risal, A.R.: Experimental investigation of minimization in surfactant adsorption and improvement in surfactant-foam stability in presence of silicon dioxide and aluminum oxide nanoparticles. J. Pet. Sci. Eng. **159**, 115–134 (2017). https://doi.org/10.1016/j.petrol.2017.09.021

83. Zargartalebi, M.; Barati, N.; Kharrat, R.: Influences of hydrophilic and hydrophobic silica nanoparticles on anionic surfactant properties: interfacial and adsorption behaviors. J. Pet. Sci. Eng. **119**, 36–43 (2014). https://doi.org/10.1016/j.petrol.2014.04.010

84. Wu, Y., et al.: Reducing surfactant adsorption on rock by silica nanoparticles for enhanced oil recovery. J. Pet. Sci. Eng. **153**, 283–287 (2017). https://doi.org/10.1016/j.petrol.2017.04.015